南京航空航天大學 | 航空学院

NANJING UNIVERSITY OF AERONAUTICS AND ASTRONAUTICS

The 23rd International Conference on Composites Materials,
July 30th-August 4th, 2023, Belfast, Northern Ireland

Simultaneous monitoring on forming pressure and residual strain of CFRP using PSFBG

C.H. Chen[1*], Q. Wu[1*], H.Z. Zhai[1], H.Q. Zhang[1], K. Xiong[1], T. Sun[2, 3] and K. T. V. Grattan[2, 3]

[1] State Key Laboratory of Mechanics and Control for Aerospace Structures, Nanjing University of Aeronautics and Astronautics, Nanjing University of Aeronautics and Astronautics, Nanjing, China
[2] Department of Electrical and Electronic Engineering, City, University of London, London, United Kingdom
[3] Sengenia Ltd., University Road, Belfast, United Kingdom

* Corresponding: chenchanghao@nuaa.edu.cn; wu.qi@nuaa.edu.cn

OUTLINE

1 Background

1.1 Carbon fiber reinforced thermoplastic (CFRTP)

Composite structures in aviation industry

Author	*Matrix*	*Performance*	*Forming process*
CFRTP	**Thermoplastic**	**Impact resistance, recyclability, short production time**	**High temperature and pressure**
CFRP	Thermosetting	High specific stiffness	Low temperature and pressure

* CFRTP: carbon fiber reinforced thermoplastic, CFRP: carbon fiber reinforced polymer

[1] http://www.comac.cc [2] https://en.wikipedia.org/wiki/General_Electric_GEnx [3] https://www.plastics.gl/automotive/composites-above-the-clouds

1 Background

1.2 Forming process

High Temperature

High Pressure

Strain/Stress

Deformation

Warpage

Warpage may lead to structural failure [4].

Forming pressure

Forming pressure affects porosity [5] and R-zone quality [6].

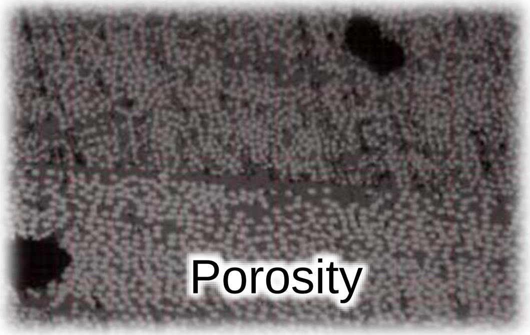

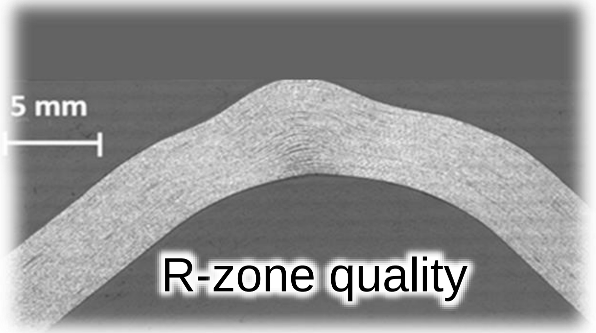

Out-of-plane strain that occurs during the forming process closely correlates with pressure and has a significant impact on product quality.

[4] Youssef Y, Denault J. *Polym Compos* 1998,19(3): 301.
[5] Zhang HQ, Wu Q*, Xiong K*, et al. *IEEE Sens J* 2022, 22(16): 15991.
[6] Belnoue J, Nixon-Pearson O, Thompson A. *J Eng Ind* 2018, 140(7), 071006.

1.3 In-plane strain and temperature monitoring using FBG

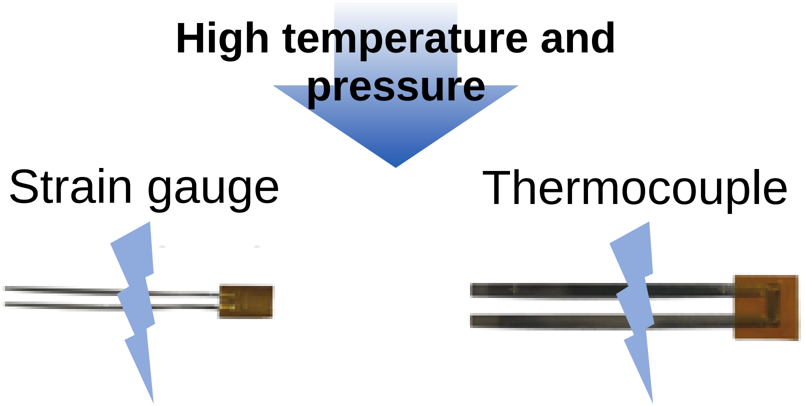

Traditional electric sensor

Accuracy affected by temperature, humidity and electromagnetic interference

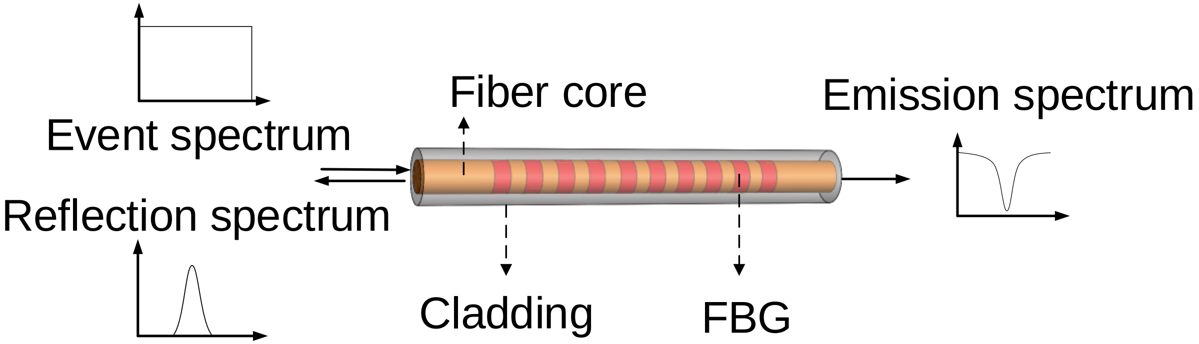

Fiber Bragg grating (FBG)

Small size, light weight, high temperature resistance, multiplexing capability, anti-electromagnetic interference

in-situ forming monitoring of CFRTP using FBG

Author	*Reinf/Matrix*	*Max. temp.* (°C)	*Max. pressure* (MPa)
Lubineau and Mulle et al. [7]	GF/PP	210	0.75
Takeda and Tsukada et al. [8]	CF/PPS	325	0.1

[7] Mulle M, Wafai H, Yudhanto A, Lubineau G*, et al. *Compos Sci Technol* 2016, 123: 143.

[8] Tsukada T*, Takeda SI, Minakuchi S, et al. *J Compos Mater* 2016, 0(0): 1-11.

1 Background

1.4 Out-of-plane strain monitoring using FBG

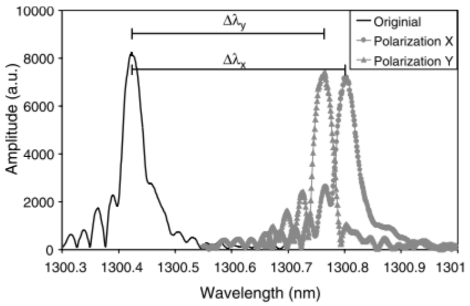

Low resolution

Meth: Birefringence

Obj: CFRP, Transverse strain difference

2005 *Sorensen and Botsis* [9]

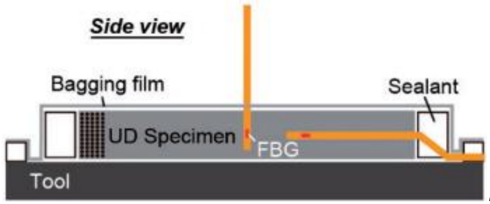

Limited applicability

Meth: Insert trough thickness

Obj: CFRP, Out-of-plane strain

2015 *Minakuchi* [11]

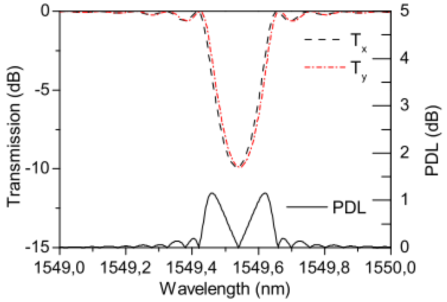

2013 *Lammens* [10]

Meth: Polarization dependent loss

Obj: CFRP, Transverse strain difference

Complex demodulation

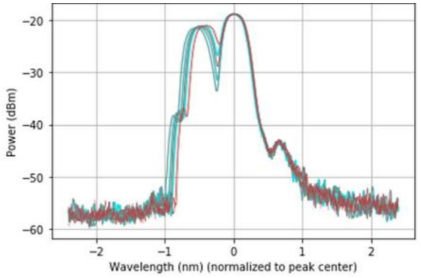

2020 *Gouws* [12]

Meth: Polarization-maintaining FBG

Obj: Transverse strain difference

Not applied in composite and Temperature dependent

There is a lack of a straightforward and precise multi-directional strain monitoring technique under the harsh conditions of CFRTP forming.

[9] Sorensen L, Gmür T, Botsis J*. *Compos Part A* 2006, 37(2): 270.
[10] Lammens N*, Kinet D, Chah K, Luyckx G, et al. *Compos Part A* 2013, 52: 38.
[11] Minakuchi S*. *J Compos Mater* 2015, 49(9): 1021.
[12] Gouws A*, Ford R K, Jones H B. *Eng Res Express* 2020, 2, 045016.

OUTLINE

2 Sensing principle

2.1 Phase-shifted fiber Bragg grating (PSFBG)

Schematic of PSFBG

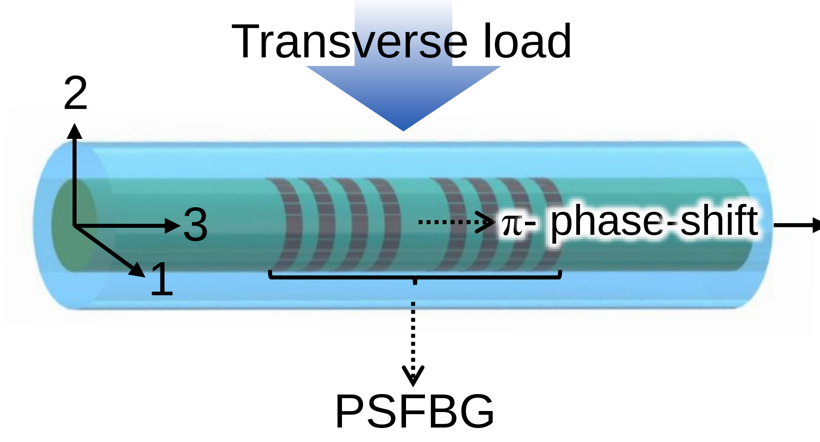

Transmission spectrum

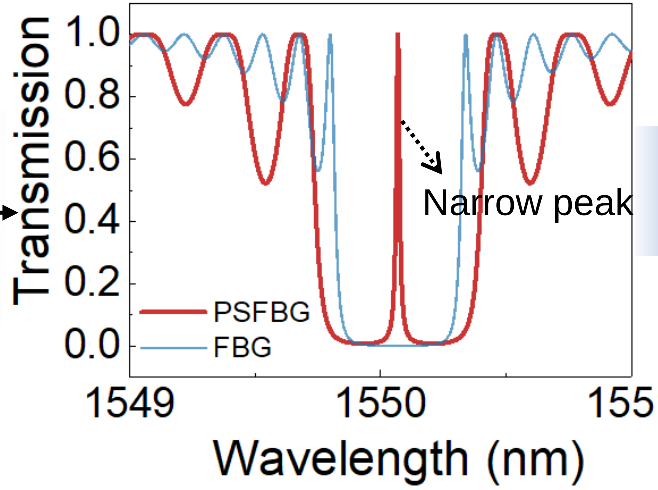

Birefringence

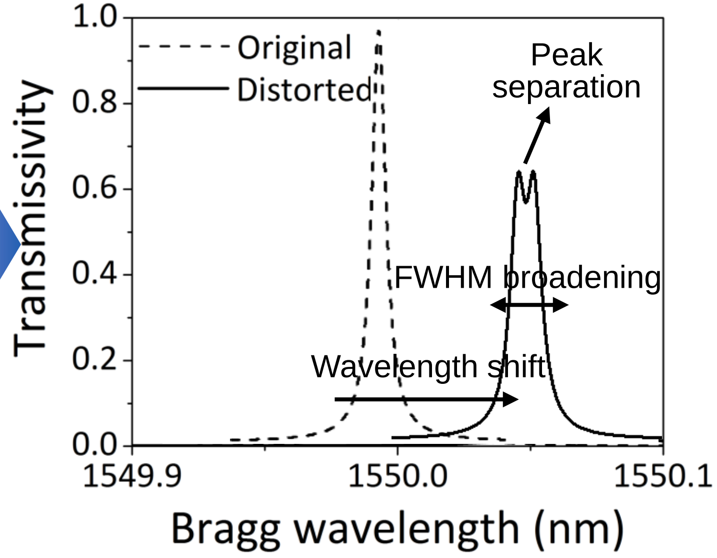

*FWHM: full-width at half-maximum

- **PSFBG has an extremely narrow transmission peak due to phase shift.**
- **Temperature and axial strain → wavelength shift.**
- **Transverse strain → birefringence.**

南京航空航天大學 NANJING UNIVERSITY OF AERONAUTICS AND ASTRONAUTICS | 航空学院

2.2 Basic equations

$$\frac{\Delta\lambda_{B,1}}{\lambda_B}=\varepsilon_3^S-\frac{n_{eff}^2}{2}[p_{11}\varepsilon_1^S+p_{12}(\varepsilon_3^S+\varepsilon_2^S)]+\xi\Delta T, \quad (1)$$

$$\frac{\Delta\lambda_{B,2}}{\lambda_B}=\varepsilon_3^S-\frac{n_{eff}^2}{2}[p_{11}\varepsilon_2^S+p_{12}(\varepsilon_3^S+\varepsilon_1^S)]+\xi\Delta T, \quad (2)$$

ε_i^S: principal strains
ΔT: temperature change
p_{11} and p_{12}: strain-optic coefficients
ξ: temperature sensitivity

Adding and subtracting Equations (1) and (2)

?

$$\boxed{\frac{\Delta\lambda_{B,1}+\Delta\lambda_{B,2}}{2}}=\kappa_1\varepsilon_3^S+\kappa_2(\varepsilon_1^S+\varepsilon_2^S)+\kappa_3\Delta T, \quad (3)$$

$$\boxed{\Delta\lambda_{B,1}-\Delta\lambda_{B,2}}=\kappa_4(\varepsilon_1^S-\varepsilon_2^S), \quad (4)$$

κ_i is constant

The derived equation indicates the correlation between spectral changes and three-directional strains.

2 Sensing principle

南京航空航天大學 | 航空学院

NANJING UNIVERSITY OF AERONAUTICS AND ASTRONAUTICS

2.3 Transfer matrix method

ΔFWHM **and peak separation vs transverse strain difference**

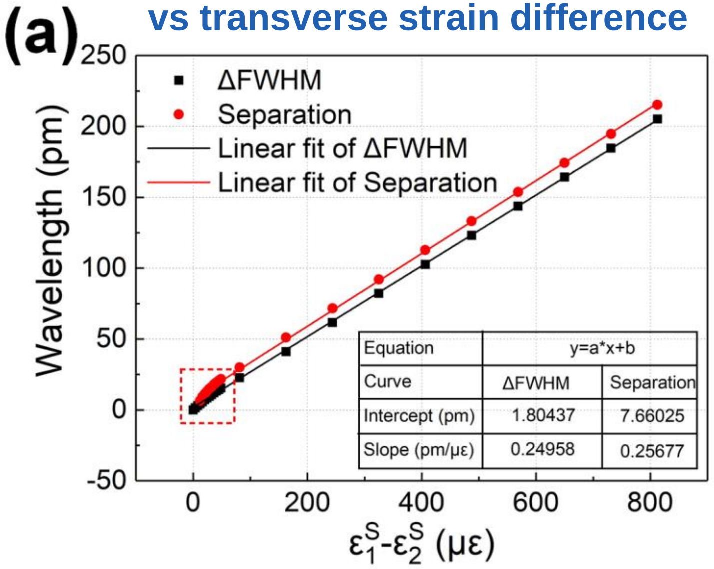

Transmission spectrum

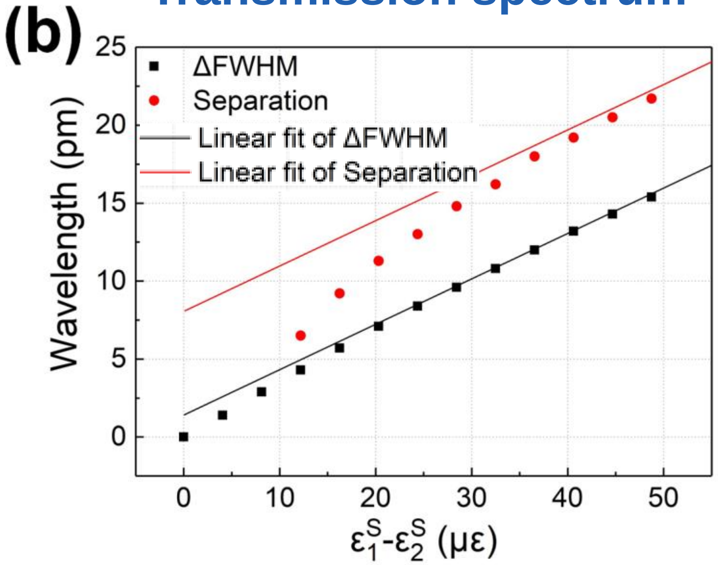

$\Delta\lambda_{B,A}$: average Bragg wavelength shift

$$\Delta\lambda_{B,A} = \frac{\Delta\lambda_{B,1} + \Delta\lambda_{B,2}}{2} = \kappa_1\varepsilon_3^S + \kappa_2(\varepsilon_1^S + \varepsilon_2^S) + \kappa_3\Delta T, \quad (6)$$

ΔFWHM: full-width at half-maximum

$$\Delta FWHM = \left|\Delta\lambda_{B,1} - \Delta\lambda_{B,2}\right| = \kappa_4\left|\varepsilon_1^S - \varepsilon_2^S\right|. \quad (7)$$

The demodulation technique using *ΔFWHM* exhibits better linearity compared to peak separation.

2.4 Interrogation method

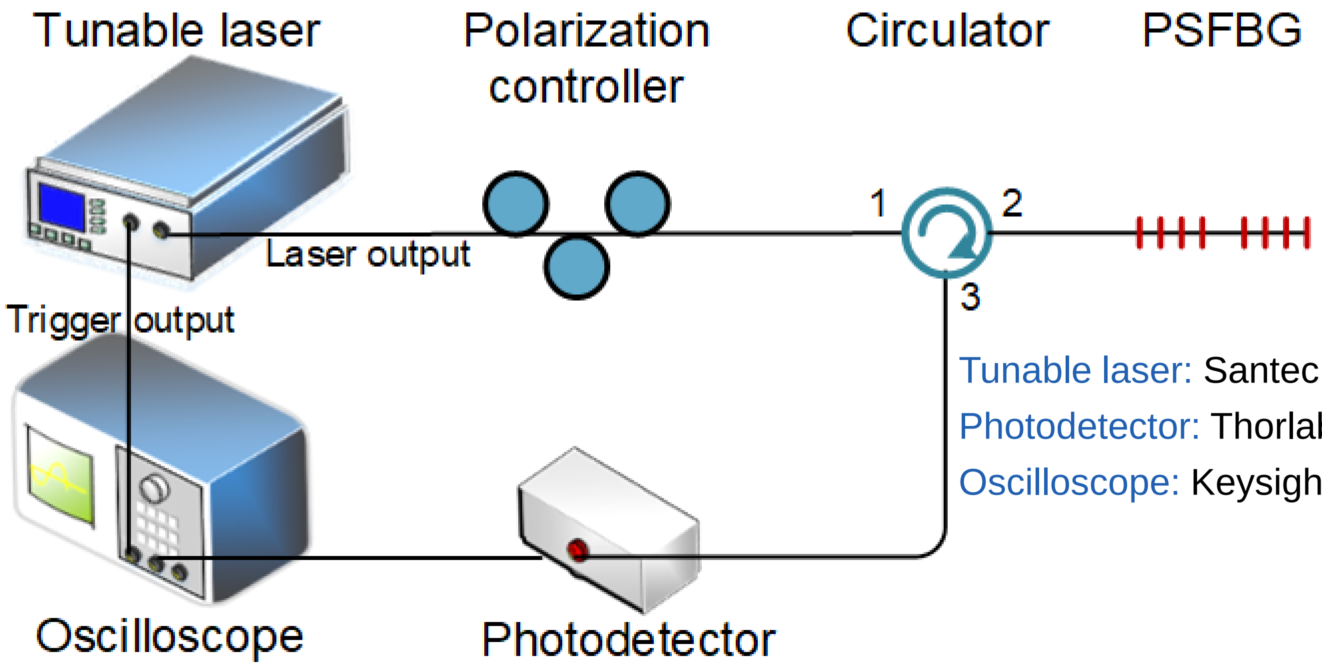

Tunable laser: Santec TSL-710
Photodetector: Thorlabs PDA10CS2
Oscilloscope: Keysight DSOX2004A

Schematic of interrogation system

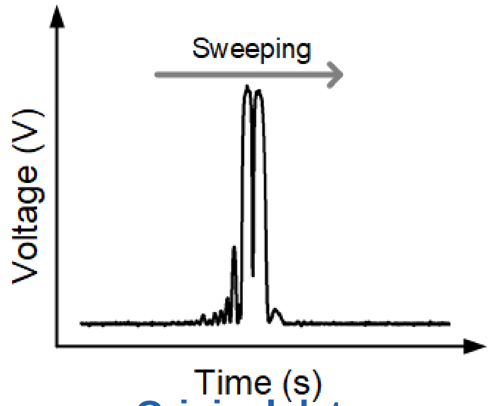

Original data

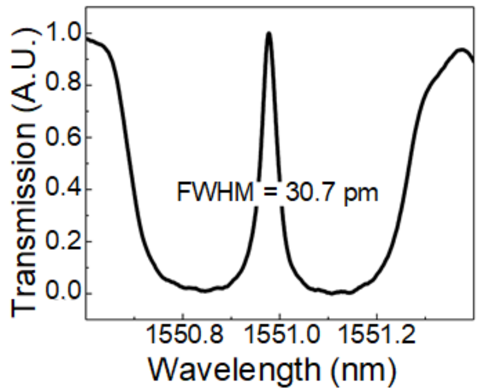

Transmission spectrum

Continuous wavelength sweep can finely characterize the narrow transmission peak of PSFBG with a resolution of 0.1 pm.

2 Sensing principle

2.5 Calibration

Temperature

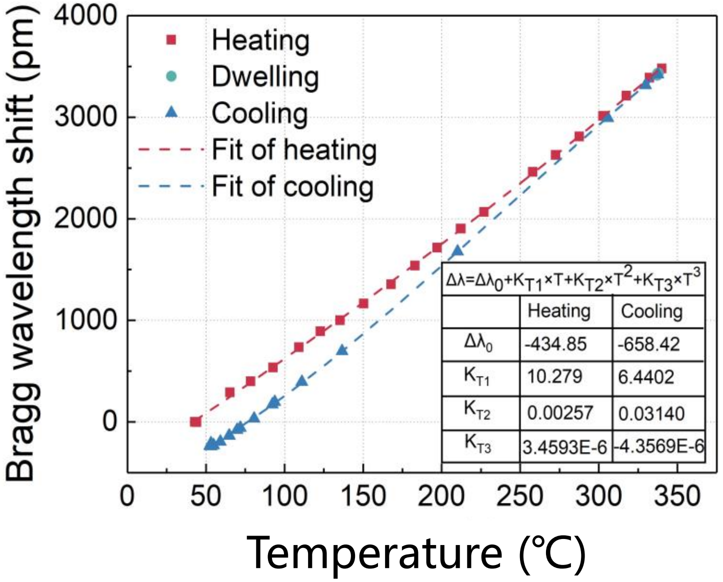

Axial strain

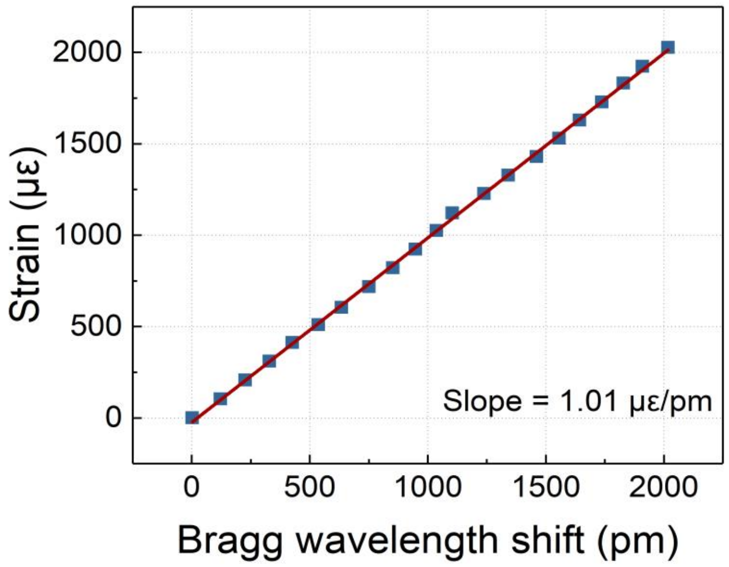

Transverse strain

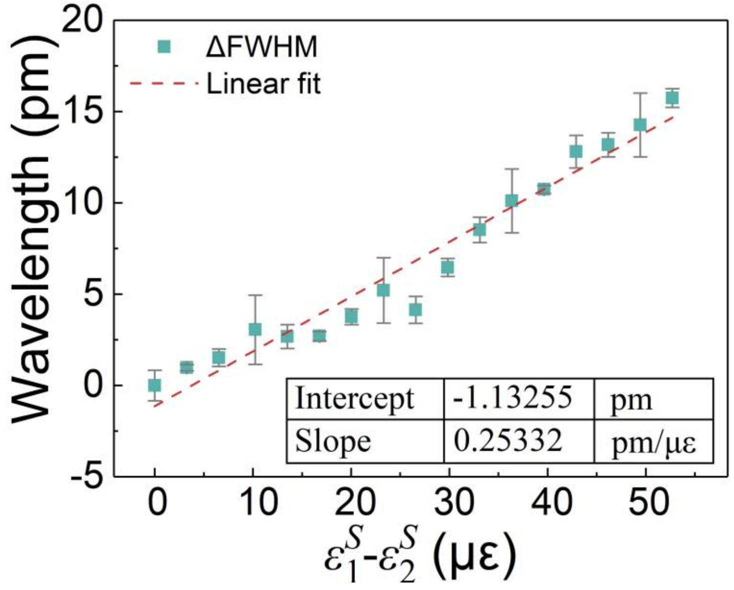

The sensitivities of temperature, axial strain, and transverse strain are calibrated before forming monitoring.

OUTLINE

3 Forming monitoring experiment

南京航空航天大學 NANJING UNIVERSITY OF AERONAUTICS AND ASTRONAUTICS | 航空学院

3.1 Sensor setup

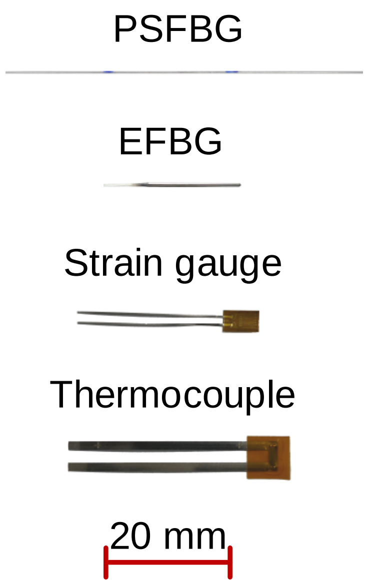

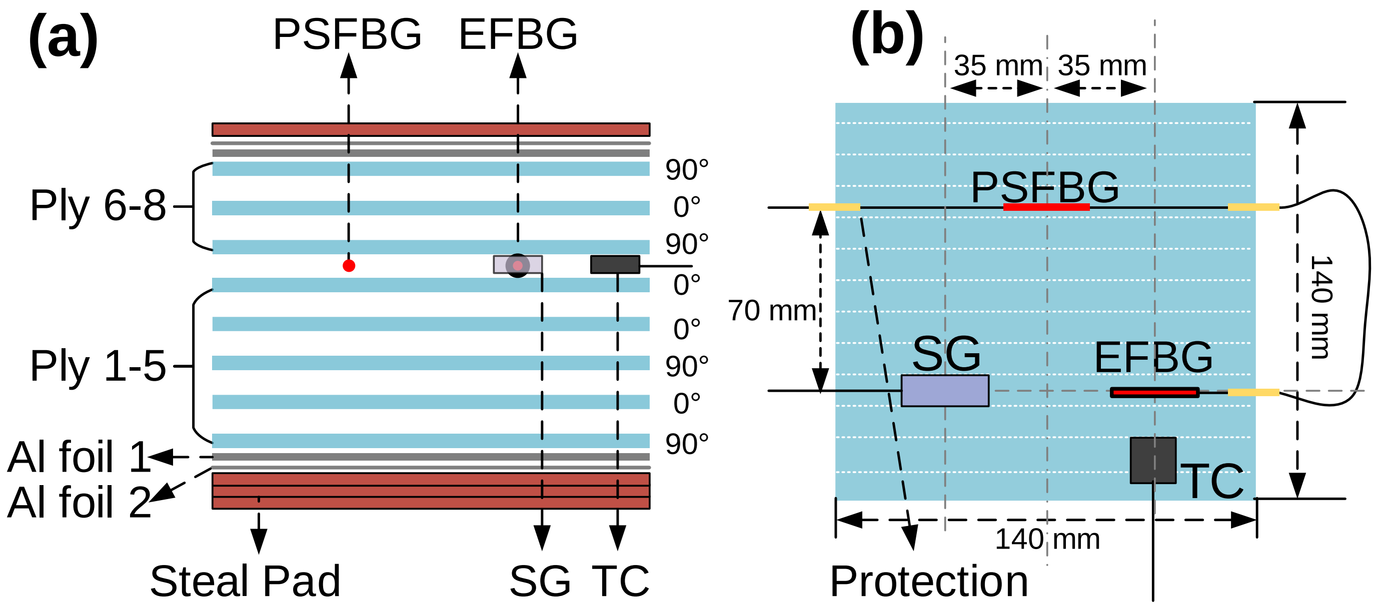

PSFBG: phase-shifted fiber Bragg grating (FYBSENSE, 1545 nm)
EFBG: encapsulated fiber Bragg grating (SHENGHAI, 1550 nm)
SG: strain gauge (KYOWA, KFU-2-120-C1-16)

TC: thermocouple (CHINO, C060-K)
Ply 1-8: CF/PEI prepregs (TORAY, Cetex TC1000 Premium)
Al foil: aluminum foil
Steal Pad: 1 mm
Protection: steel capillary

3 Forming monitoring experiment

南京航空航天大學 NANJING UNIVERSITY OF AERONAUTICS AND ASTRONAUTICS 航空学院

3.2 Forming process

Process curve

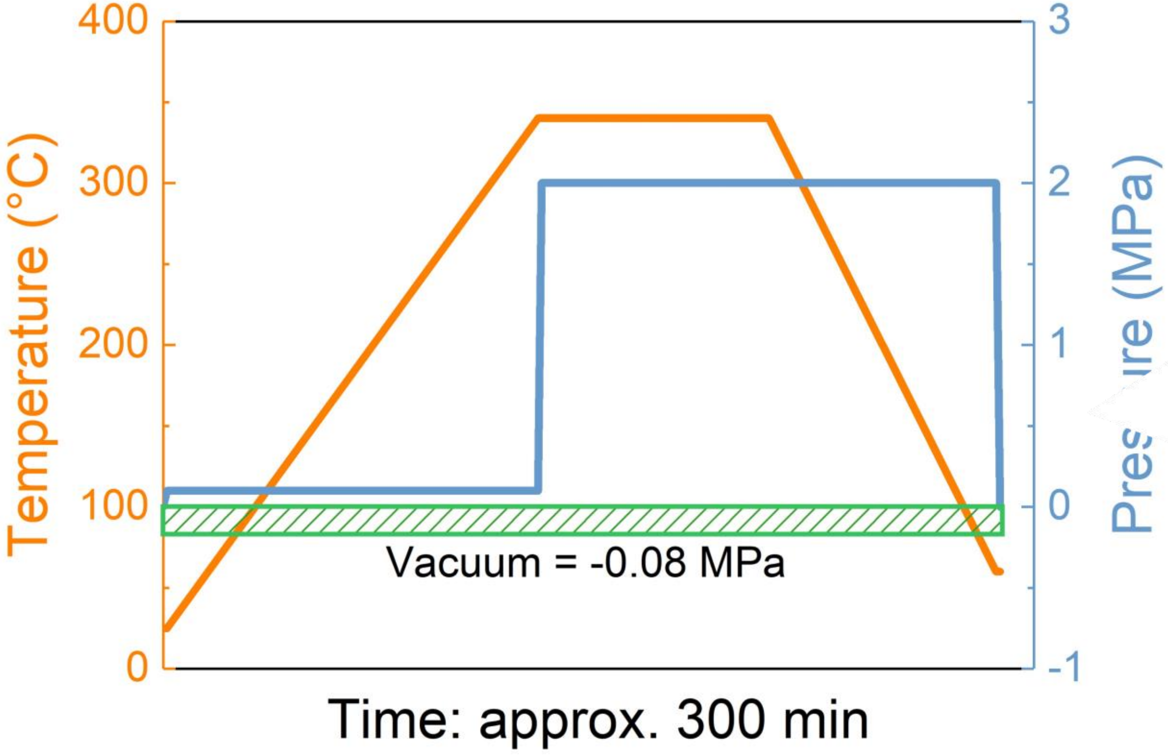

Manufactured laminate

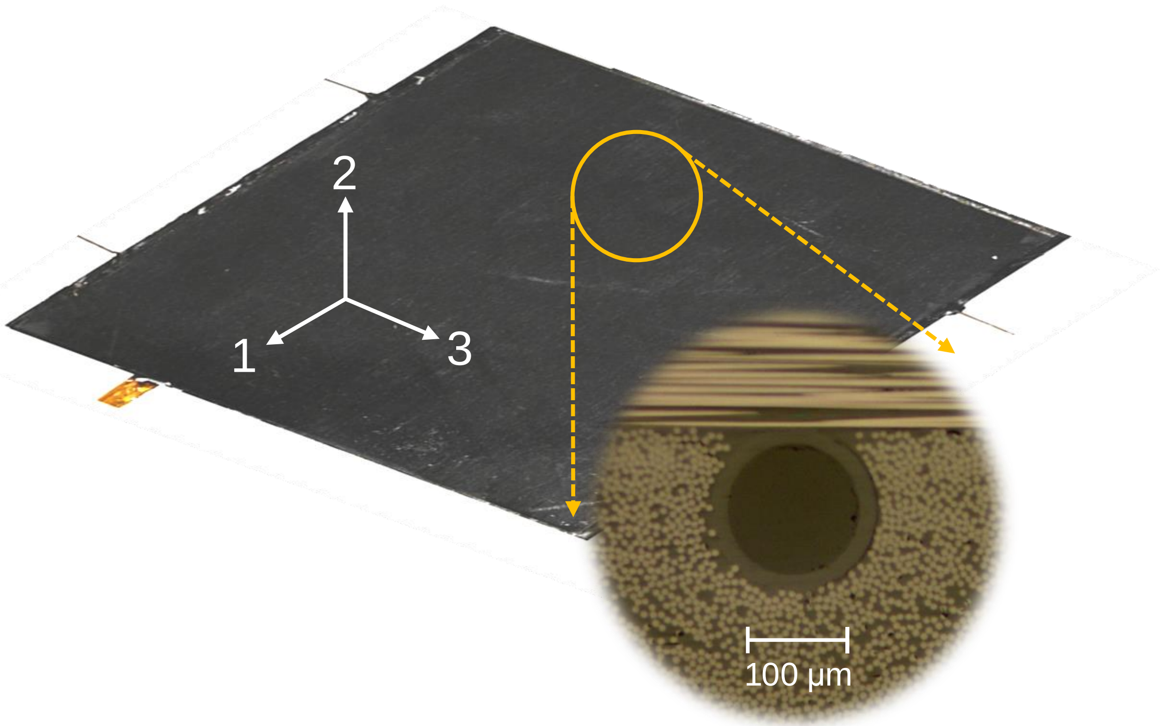

The CFRTP laminate exhibits a smooth surface and high quality.
No obvious resin rich area can be observed.

3 Forming monitoring experiment

3.3 Spectra

T_{ll}: liquid-liquid transition temp. (rubbery-viscous transition temp.)

Temperature dependent modulus of PEI

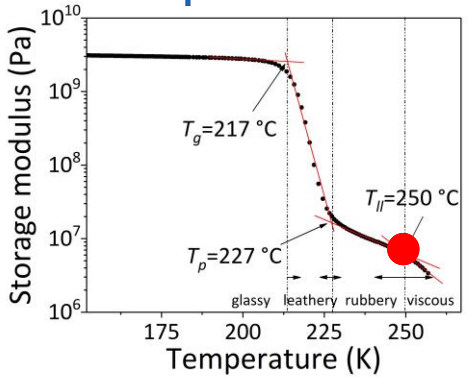

I: Heating from T_r ~ T_{ll}

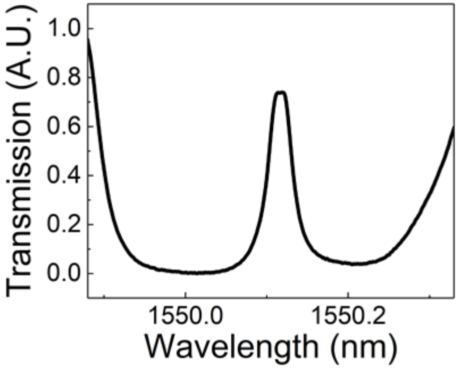

II: Heating from T_{ll} ~ 340 ℃

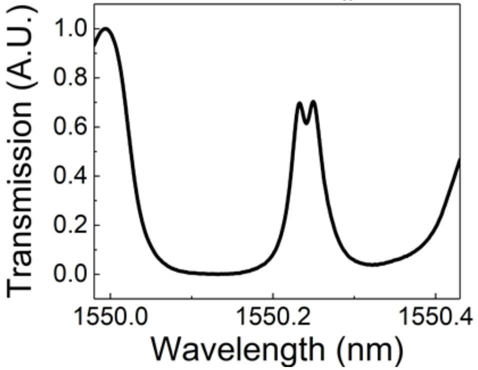

III: Dwelling

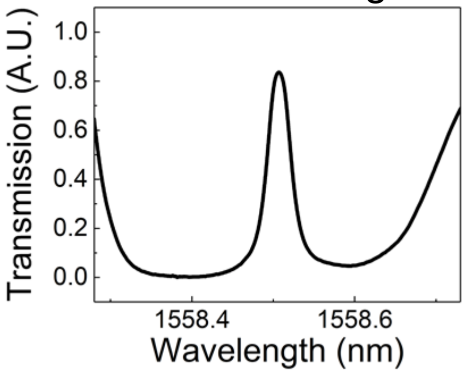

IV: Cooling from 340 ℃ ~ T_{ll}

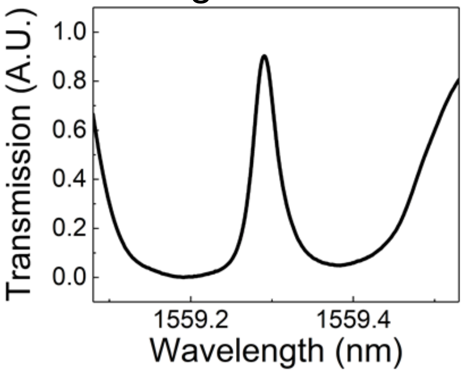

V: Cooling from T_{ll} ~ T_r

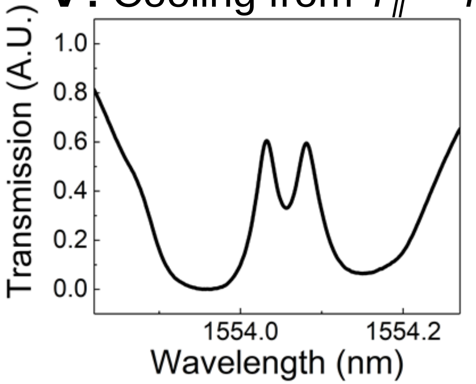

ε_3^S and $\left|\varepsilon_1^S - \varepsilon_2^S\right|$ can be determined based on the wavelength shift and *ΔFWHM* of the transmission peak.

3 Forming monitoring experiment

南京航空航天大學 | 航空学院
NANJING UNIVERSITY OF AERONAUTICS AND ASTRONAUTICS

3.4 Temperature monitoring

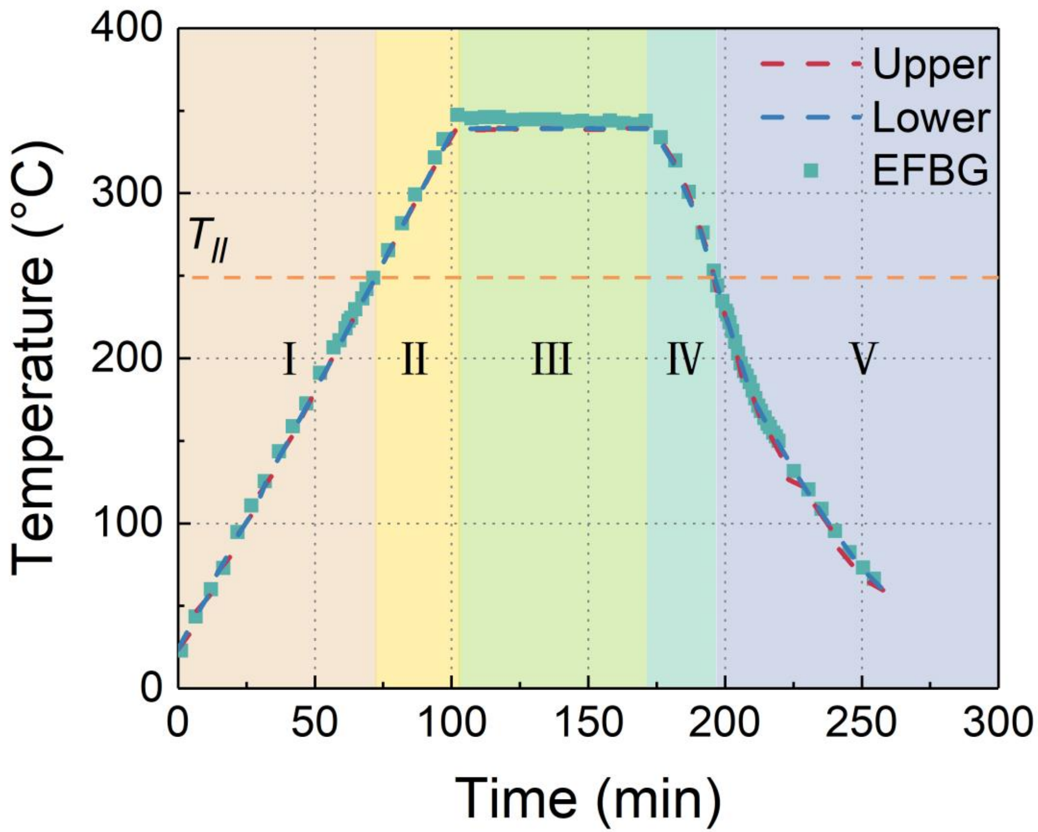

The forming temperature can be precisely monitored with an average difference of 3 ℃ compared to the TC.

3 Forming monitoring experiment

3.5 Axial strain monitoring

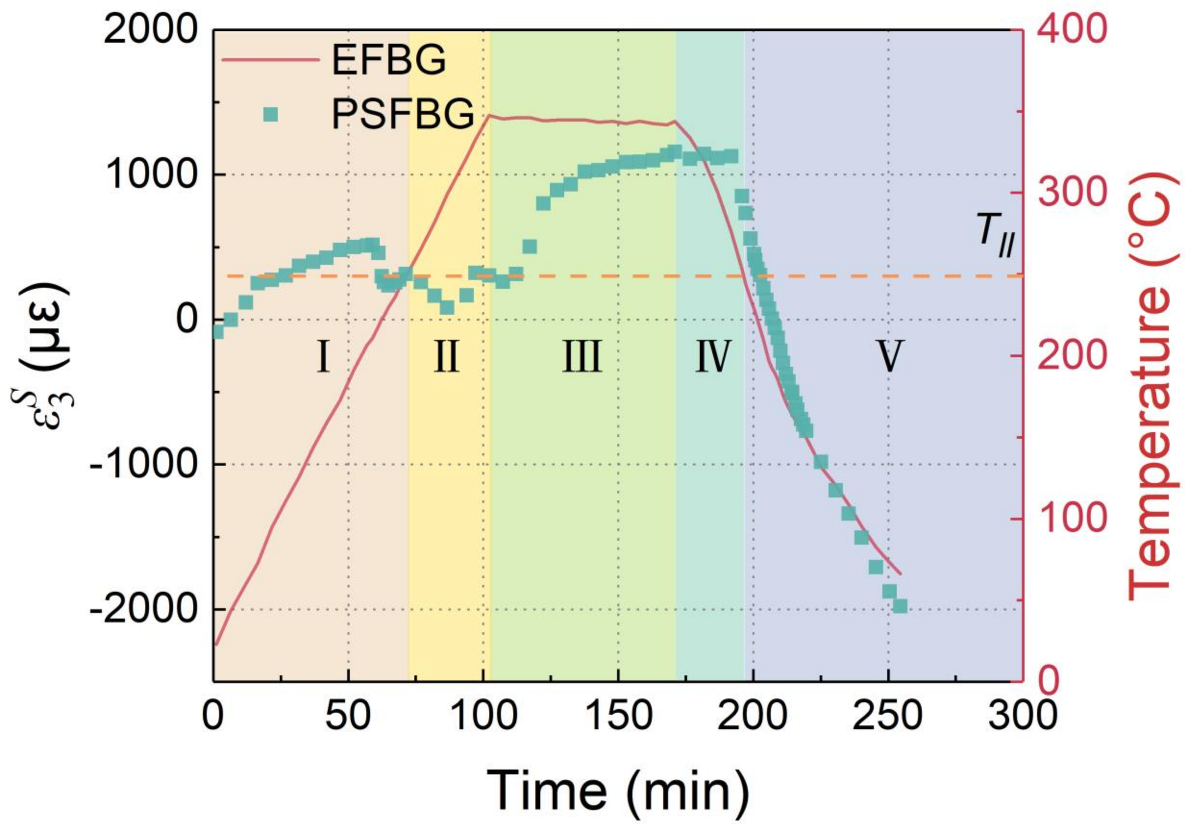

The axial residual strain can be precisely monitored with an average difference of 92 με compared to the FBG during the cooling phase.

3.6 Transverse strain monitoring

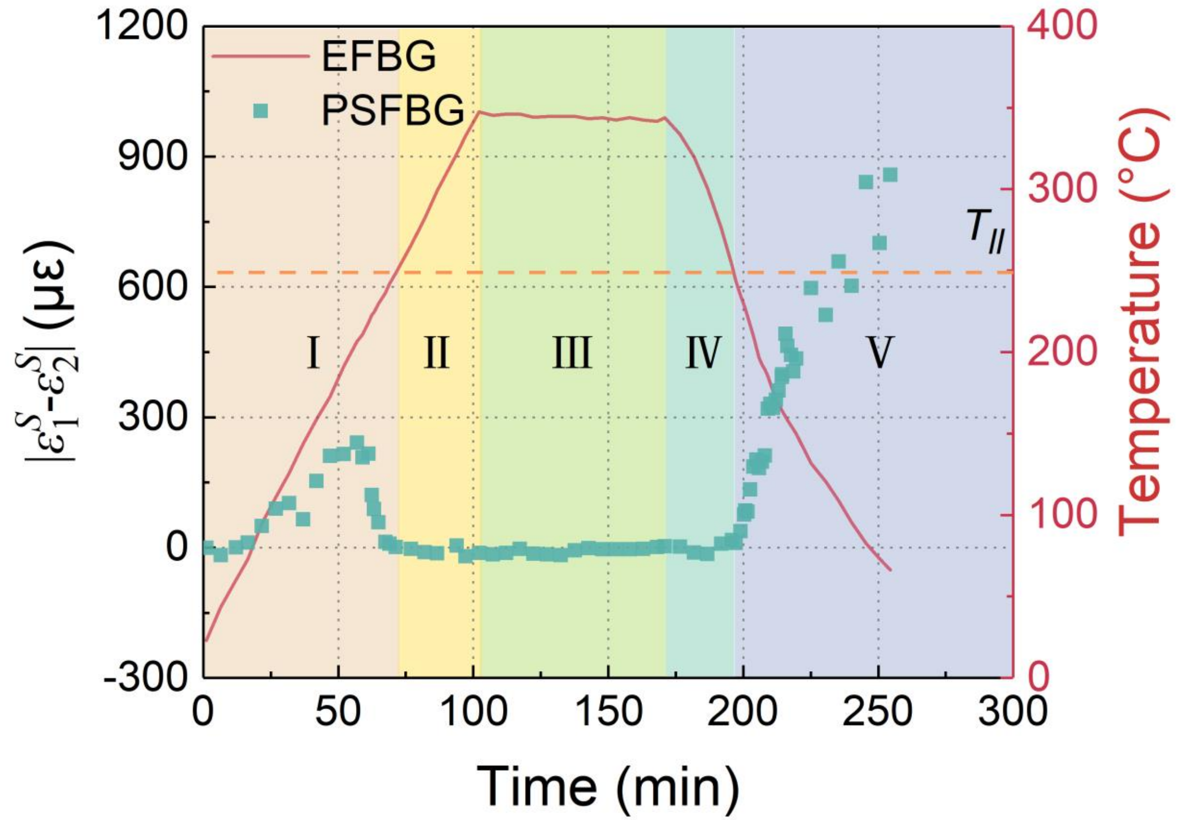

The transverse residual strain difference can be monitored with a similar trend to the force sensor.

3 Forming monitoring experiment

南京航空航天大學 NANJING UNIVERSITY OF AERONAUTICS AND ASTRONAUTICS | 航空学院

3.7 Strain vs temperature

Axial strain

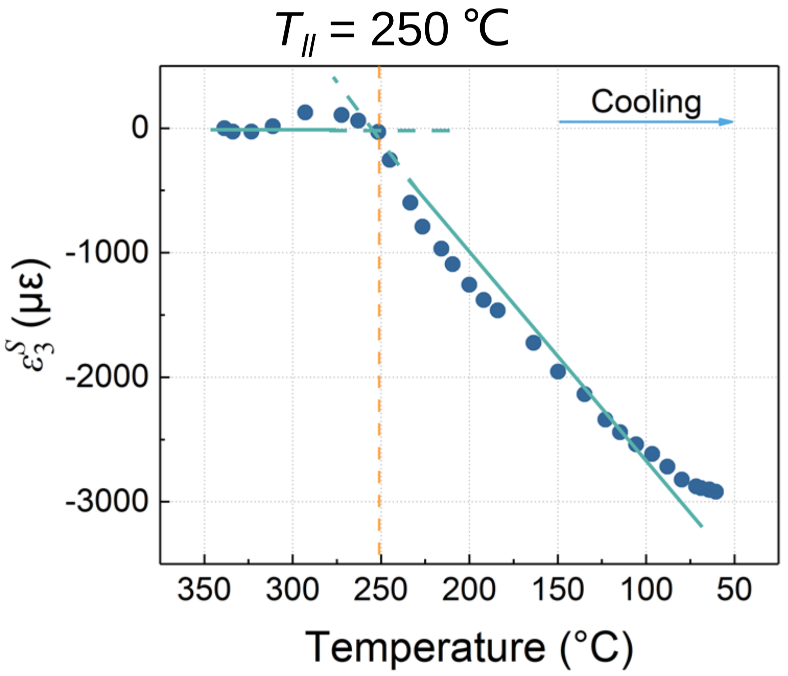

Transverse strain difference

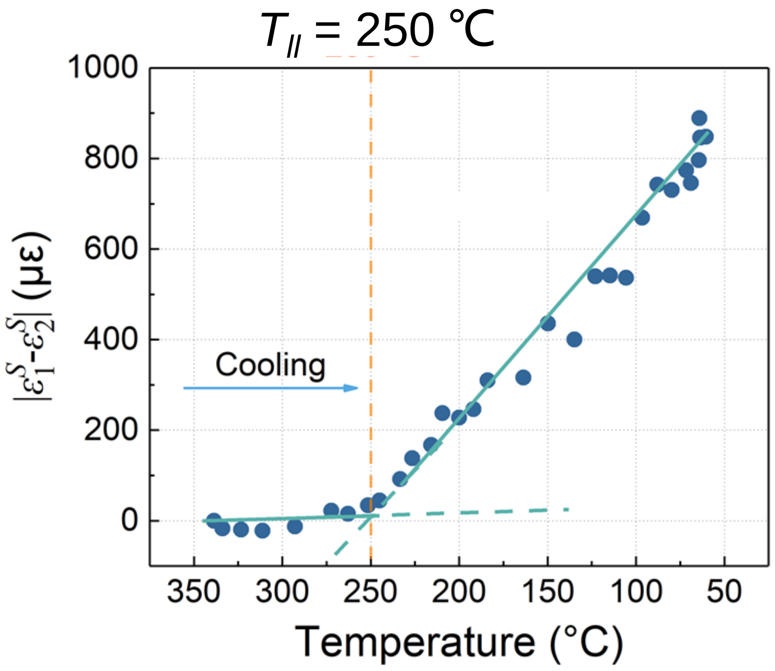

Schematic of interfacial bonding

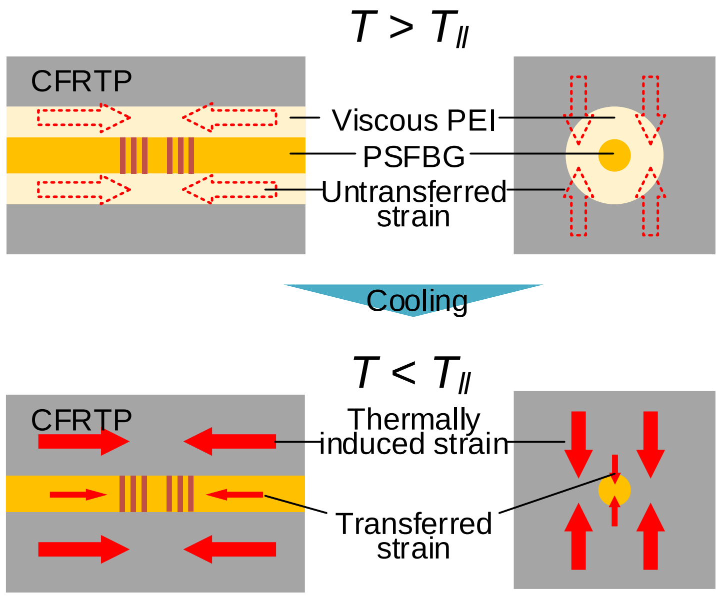

The knee points of both ε_3^S and $\left|\varepsilon_1^S - \varepsilon_2^S\right|$ occur at $T_{//}$, which can be attributed to enhanced interfacial bonding.

OUTLINE

5 Thermomechanical analysis

南京航空航天大學 NANJING UNIVERSITY OF AERONAUTICS AND ASTRONAUTICS | 航空学院

5.1 Finite element model

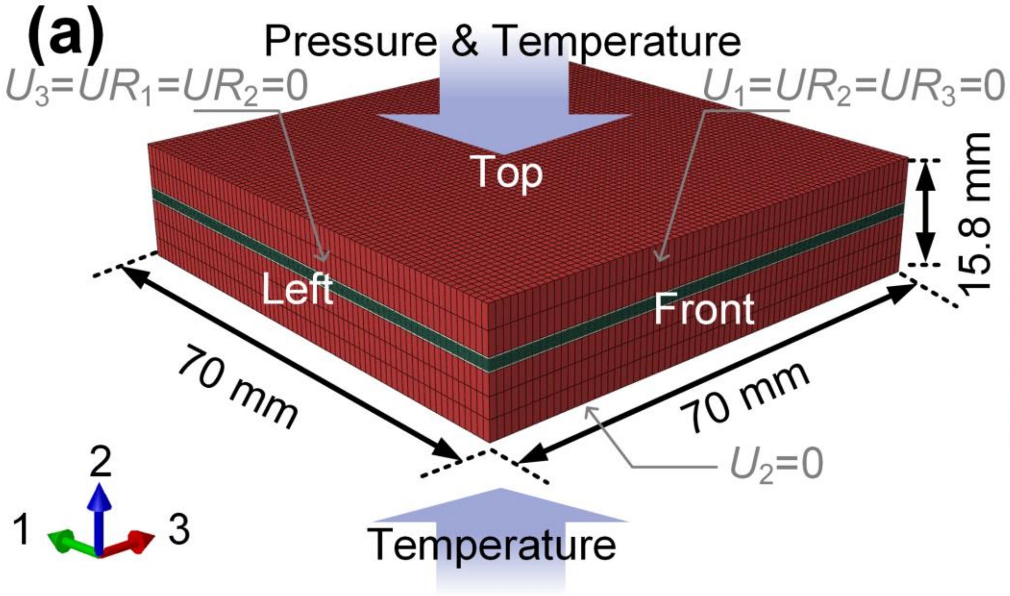

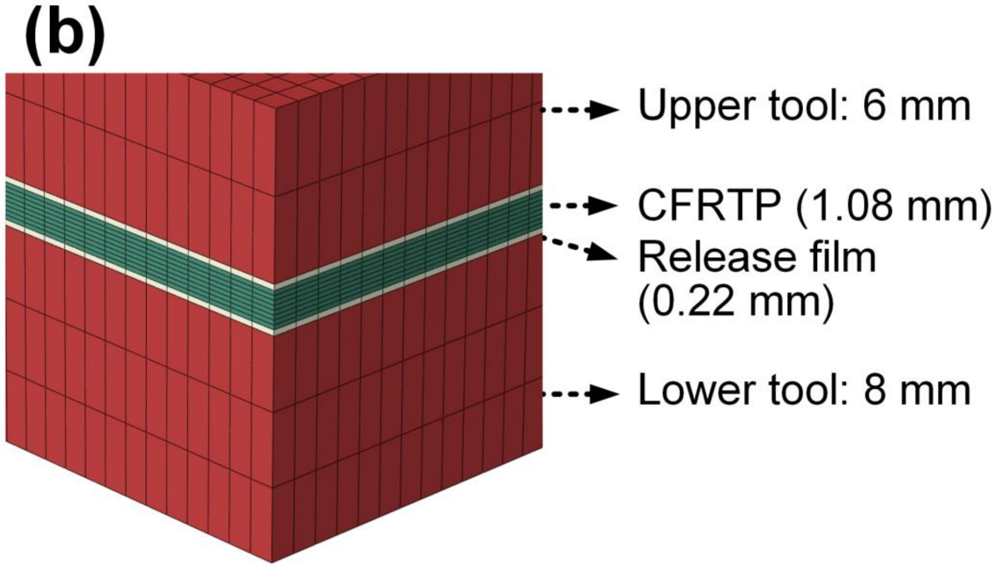

Material properties

Part	*Material*	ρ (t/mm³)	C_p (mJ·K⁻¹t⁻¹)	k (mW·mm⁻¹K⁻¹)	E (MPa)	ν	α (K⁻¹)
Tool	Steel	8.03×10^{-9}	5×10^{8}	16.3	193000	0.29	18.4×10^{-6}
Shear layer	Al	2.73×10^{-9}	9.2×10^{8}	19.3	70000	0.33	24×10^{-6}
CFRTP	CF/PEI	**Homogenized, temperature dependent, orthotropic** material properties [13]					

Mesh

Item	*Value*
Element	C3D20RT
Global size	1 mm
Node num	315311

[13] Zhai HZ, Wu Q*, Yoshikawa N, Xiong K, Chen CH, et al. *J Compos Mater* 2023, 0(0), 1-22.

5.2 Strain distribution

The impact of CFRTP residual strain on PSFBG spectra is investigated based on the simulation results.

Strain distribution in ply 5 containing the PSFBG

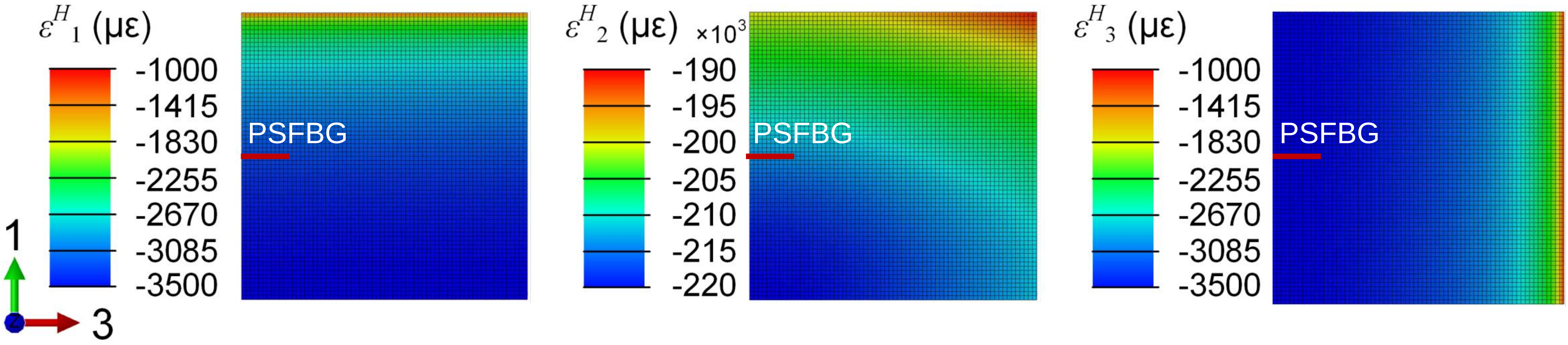

In-plane strains converge to asymptotic values from edges to the center, while the out-of-plane strain exhibits a radial distribution.

5 Thermomechanical analysis

5.3 Strain comparison

Simulated strain

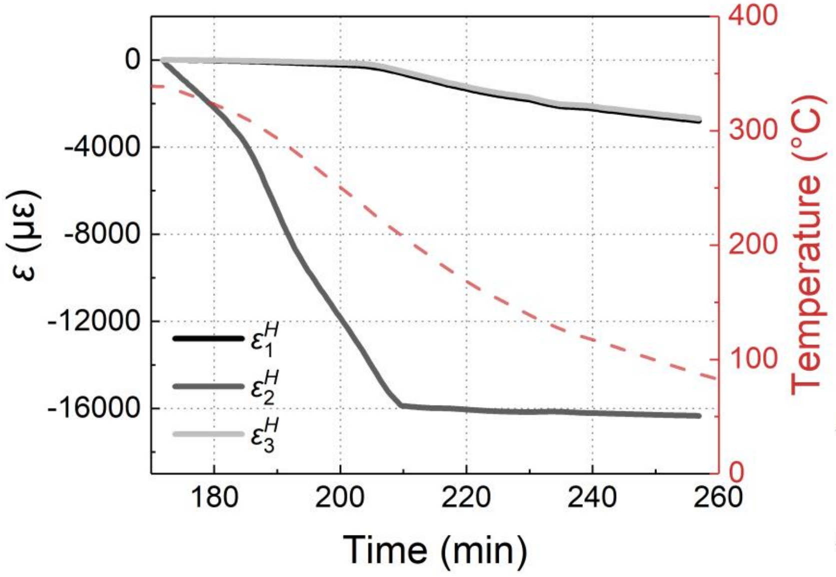

The simulated in-plane strains are nearly equal:

$$\varepsilon_1^H \approx \varepsilon_3^H$$

The axial strain of PSFBG correlates with the simulation results.

Axial strain

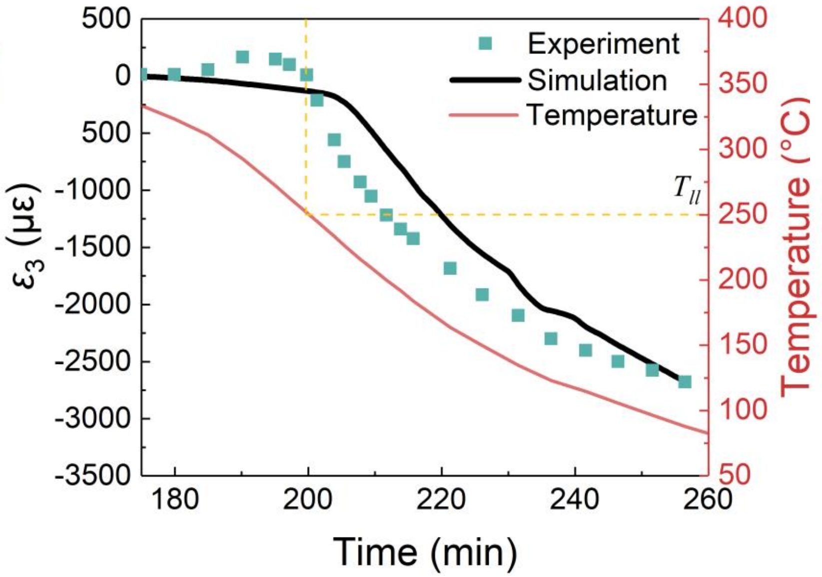

Transverse strain difference

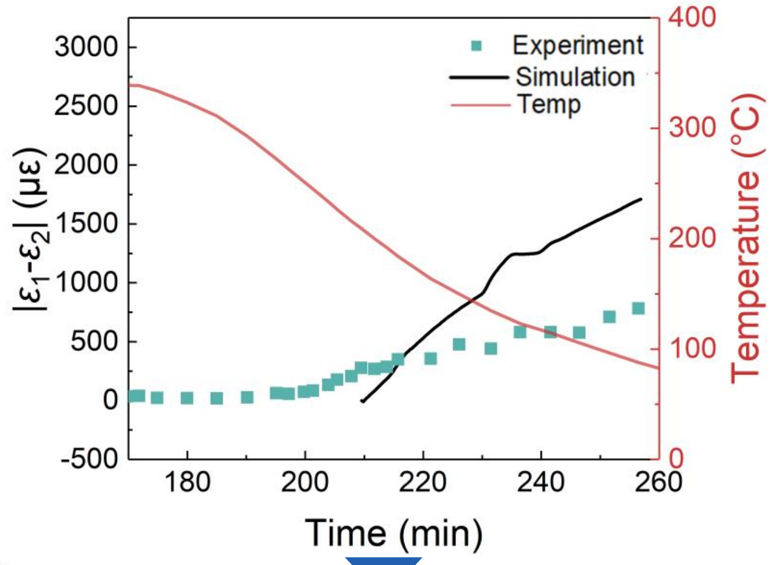

The transverse strain difference shows a similar trend to the simulation but noticeable different value.

OUTLINE

6 Conclusion

01 *PSFBG characteristics for CFRTP forming monitoring*

Wavelength shift exhibits a cubic relation with temperature and linear relation with axial strain. FWHM exhibits a linear relation with transverse strain difference.

02 *Strain transfer and decoupling*

Strain relation between CFRTP and PSFBG is characterized by a strain transfer matrix, deriving the three-directional strain decoupling method.

03 *Temperature and three-directional strain monitoring*

Temperature shows a difference of 3 ℃ compared to TC. ε_3^H shows a difference of 92 με compared to FBG. ε_1^H and ε_2^H show max. difference of 124 με compared to simulation.

04 *Forming pressure characterization*

Out-of-plane strain of CFRTP exhibits higher contraction under higher forming pressure, enabling the potential for forming pressure monitoring.

* Funding and acknowledgement

Funding

National Key R&D Program of China (2021YFF0501800).

National Natural Science Foundation of China (11972016, 12111530106).

Fund of State Key Laboratory of Mechanics and Control for Aerospace Structures (MCMS-I-0521G04).

Acknowledgement

Prof.
Qi Wu

Prof.
Ke Xiong

Prof.
Kenneth Grattan
OBE FREng

Prof.
Tong Sun
OBE FREng

Prof.
Yoji Okabe

Prof.
Nobuhiro Yoshikawa

THANK YOU FOR LISTENING